Incremental Nonlinear Dynamic Inversion Control for Hydraulic Hexapod Flight Simulator Motion Systems

Huang, Yingzhi; Pool, D. M.; Stroosma, O.; Chu, Q. P.

DOI
10.1016/j.ifacol.2017.08.837

Publication date
2017

Document Version
Final published version

Published in
IFAC-PapersOnLine

Available online at www.sciencedirect.com

ScienceDirect

IFAC Papers Online CONFERENCE PAPER ARCHIVE

IFAC PapersOnLine 50-1 (2017) 4294–4299

Incremental Nonlinear Dynamic Inversion Control for Hydraulic Hexapod Flight Simulator Motion Systems ⋆

Yingzhi Huang, * **D.M. Pool,** * **O. Stroosma** * **and Q.P. Chu** *

* *Faculty of Aerospace Engineering, Delft University of Technology, Kluyverweg 1, 2629HS, Delft, The Netherlands. (e-mail:{Y.Huang-2,D.M.Pool,O.Stroosma,Q.P.Chu }@tudelft.nl).*

Abstract: Hydraulic driven manipulators face serious control problems due to the nonlinear system dynamics and model and parametric uncertainties of hydraulic actuators. In this paper, a novel sensor-based Incremental Nonlinear Dynamic Inversion controller is applied to force tracking control of hydraulic actuators of a hexapod flight simulator motion system, which together with an outer-loop motion tracking controller forms a motion control system. Due to the use of feedback of pressure difference derivatives, the proposed technique is not dependent on accurate model and parameters, which makes the controller inherently robust to model uncertainties. Furthermore, The sensor-based control approach is particularly suitable for hydraulic force tracking in existence of an outer-loop controller decoupling hydraulic-mechanic interaction term from the inner-loop dynamics. Simulation results indicate that the novel approach yields better tracking performance and confirm the greater robustness to model and parametric uncertainties compared with a traditional nonlinear dynamic invention approach.

Keywords: Motion Control Systems, Mechatronic systems, Design methodologies

1. INTRODUCTION

Stewart platforms (Stewart, 1965), also known as hexapod parallel manipulators, are adopted by most modern flight simulators used for pilot training and research as motion systems due to their high stiffness and accuracy. A moving upper platform is connected to a fixed base platform with six linear actuators that provide a motion in six-degrees-of-freedom (DOF). As high actuation forces are required by larger flight simulator motion platforms, hydraulic actuators are commonly used owning to their high loading capabilities, rapid responses and, even more important, smoothness (Koekebakker, 2001). A representation of such system is the SIMONA Research Simulator (SRS) at TU Delft (Stroosma et al., 2003), as shown in Fig. 1. The increasing fidelity requirement of modern flight simulators asks for higher performance controller for the integrated motion systems.

The Stewart platform control problem has been studied extensively during the past decades. Various model-based control schemes such as computed torque control have been proposed to deal with the highly nonlinear mechanical dynamics (Chin et al., 2008). Advanced controllers like adaptive control and robust control are also studied to overcome model and parameter uncertainty problems. However, all these techniques are difficult to be applied to hydraulic manipulators directly since hydraulic actuators are not readily available force generators, and the highly nonlinear dynamics heavily interact with the hexapod mechanics. One often applied solution to this problem

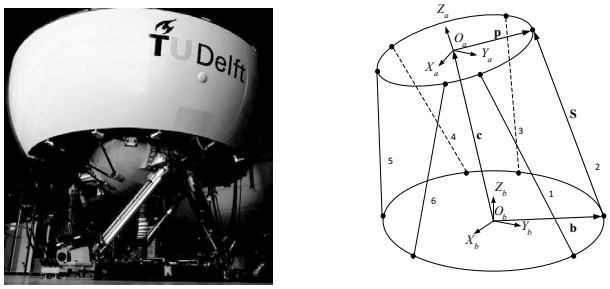

Fig. 1. A Stewart platform based motion system SRS at TU Delft and a schematic drawing

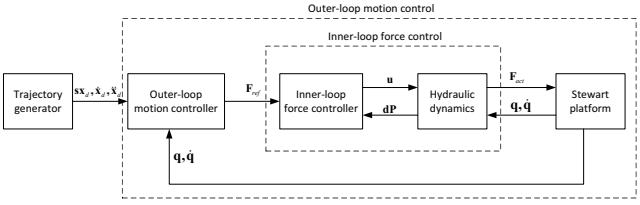

Fig. 2. Cascade control architecture for hydraulic parallel robots

is cascading the controller into a multi-loop structure as shown in Fig. 2. An inner-loop hydraulic force controller is designed to decouple the hydraulic dynamics from mechanics while generating the actuation forces calculated by a typical outer-loop robot motion controller. A high-performance hydraulic force controller is of great importance for the overall motion control performance.

⋆ The first author is sponsored by Chinese Scholarship Council.

10.1016/j.ifacol.2017.08.837

The hydraulic force control problem is challenging due to the highly nonlinear actuator dynamics (Merritt, 1967) and model uncertainties including valve opening overlaps, oil leakage and temperature-sensitive oil modulus. As pointed out in (Alleyne et al., 1998), a PID controller is inadequate for hydraulic force tracking due to fundamental limitations, which makes more advanced control schemes like nonlinear dynamic inversion (NDI) necessary. One example is the Cascade ΔP controller (CdP) introduced in (Heintze and van der Weiden, 1995) and currently implemented in the SIMONA Research Simulator at TU Delft. However, as it is an NDI-based approach, the performance of the CdP controller is strongly influenced by hydraulic parameter uncertainties. In this context, a high performance and less model dependent hydraulic force controller is required.

The novel Incremental Nonlinear Dynamic Inversion (INDI) is a less model dependent and more robust technique that has recently been adopted for various control applications (Smeur et al., 2015; Simplício et al., 2013; Sieberling et al., 2010). By calculating the increment of the control input based on the feedback of a state derivative measurement, instead of computing the total command with the modeled state derivatives with an NDI technique, the INDI controller uses less model information and is insensitive to model and parameter uncertainties. Taking advantage of pressure sensor measurement on hydraulic systems, the application of INDI on a single hydraulic actuator was recently discussed in (Huang et al., 2016a), while a detailed controller design with INDI technique on hydraulic manipulators is still to be performed.

In this paper, the INDI control methodology is adopted to design the inner-loop force tracking controller for hydraulic actuators, which together with a traditional outer-loop force computation controller form the complete control system for a hydraulic hexapod flight simulator motion system. Numerical simulations are implemented on a well-validated and fully nonlinear model of the SRS at TU Delft. Using simulation data, robustness of the applied controller against hydraulic model and parameter uncertainties are explicitly investigated and compared with an NDI based-CdP controller.

The paper is organized as follows. Section 2 discusses the model of the hydraulic hexapod motion system. Section 3 introduces the concept of the novel INDI approach, while the detailed application of INDI to the discussed motion system is presented in Section 4. Simulation results under nominal conditions and robustness tests with model mismatches are presented in Section 5. The main conclusions are then summarized in Section 6.

2. SYSTEM DYNAMICS

2.1 Motion-Base Dynamics

The Stewart platform is a 6-DOF parallel manipulator as shown in Fig. 1. A Newton-Euler formulation (Dasgupta and Mruthyunjaya, 1998) is adopted to derive the nonlinear dynamic equations in Cartesian space. The complete system dynamics are described in closed form by a second-order nonlinear differential equation, given by:

$$\mathbf{M}(\mathbf{sx})\,\ddot{\mathbf{x}} + \boldsymbol{\eta}(\dot{\mathbf{x}}, \mathbf{sx}) = \mathbf{HF} \tag{1}$$

where $\mathbf{sx} \in \mathbb{R}^6$ is the system position vector described by upper platform origin position and orientation with respect to the lower platform and $\dot{\mathbf{x}} \in \mathbb{R}^6$ is the system velocity vector described by upper platform origin velocity and angular velocity. Note that $\dot{\mathbf{sx}}$ is not equal to $\dot{\mathbf{x}}$ since the orientation is described by Euler angles and their derivatives are not angular velocity components. $\mathbf{M} \in \mathbb{R}^{6\times6}$ is the manipulator mass matrix, $\boldsymbol{\eta} \in \mathbb{R}^6$ contains the Coriolis/centripetal terms and the gravitational term, $\mathbf{F} \in \mathbb{R}^6$ denotes the stacked actuation forces and $\mathbf{H} \in \mathbb{R}^{6\times6}$ is the transpose of the manipulator Jacobian matrix. The readers are referred to (Huang et al., 2016b) for details.

2.2 Hydraulic Actuator Dynamics

The symmetrical hydraulic actuator driven by a typical servo valve is depicted in Fig. 3. The actuation force is generated on the moving piston with the oil pressure difference $P_{p1} - P_{p2}$ between the two separated chambers. Consider the oil flow coming into and out of the two actuator cylinder compartments, the pressure dynamics of each chamber is obtained by describing the oil compressibility with the following equations

$$\begin{aligned} \dot{P_{p1}} &= \frac{E}{V_1}\left(\Phi_{p1} - \Phi_{lp} - \Phi_{l1} - A_p\dot{q}\right) \\ \dot{P_{p2}} &= \frac{E}{V_2}\left(-\Phi_{p2} + \Phi_{lp} + \Phi_{l2} + A_p\dot{q}\right) \end{aligned} \tag{2}$$

where q is the actuator length, Φ_{p1} and Φ_{p2} are the oil flows controlled by the servo-valve, Φ_{l1}, Φ_{l2} and Φ_{lp} are the leakage flows illustrated in Fig. 3, V_1 and V_2 are the cylinder volumes of both chambers, A_p is the piston area and E denotes the oil bulk modulus.

In order to describe the pressure dynamics of Eq. (2) in a single equation, a change of coordinates is applied as in (Koekebakker, 2001)

$$\begin{bmatrix} P_m & \Phi_m & \Phi_{lm} & C_m \\ dP & d\Phi & d\Phi_l & dC \end{bmatrix} = \begin{bmatrix} \frac{1}{2} & \frac{1}{2} \\ 1 & -1 \end{bmatrix} \begin{bmatrix} P_{p1} & \Phi_{p1} & \Phi_{l1} & E/V_1 \\ P_{p2} & \Phi_{p2} & \Phi_{l2} & E/V_2 \end{bmatrix} \tag{3}$$

Thus Eq. (2) can be transformed to

$$\dot{dP} = 2C_m\left(\Phi_m - \Phi_{lm} - \Phi_{lp} - A_p\dot{q}\right) + \frac{dC}{2}\left(d\Phi - d\Phi_l\right) \tag{4}$$

Neglecting the small second term and assuming the leakage flow to be laminar and is proportional to the pressure difference, a simplified pressure dynamics equation can be written as

$$\dot{dP} = 2C_m\left(\Phi_m - L_{lm}dP - A_p\dot{q}\right) \tag{5}$$

Under assumptions that the valve geometry is ideal with a perfectly symmetric configuration, the controlled oil supply flow Φ_m is obtained as (Merritt, 1967)

$$\Phi_m = \frac{\Phi_{p1} + \Phi_{p2}}{2} = C_d h_m x_m \sqrt{\frac{P_s}{\rho}\left(1 - \frac{x_m}{|x_m|}\frac{dP}{P_s}\right)} \tag{6}$$

where x_m is the valve spool displacement, C_d is the discharge coefficient and h_m is the width of the spool port opening.

Defining the maximum flow as $\Phi_n = C_d h_m x_{m,max}\sqrt{P_s/\rho}$, which represents the controlled flow with maximum valve

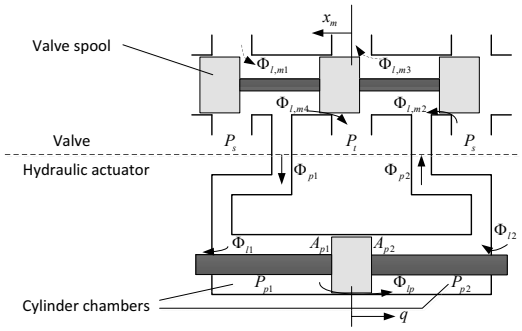

Fig. 3. A hydraulic actuator driven by a valve

spool displacement and zero pressure difference, Eq. (6) can be substituted in Eq. (5) and give

$$\dot{dP} = C_m \left(\Phi_n \sqrt{1 - \frac{x_m}{|x_m|} \frac{dP}{P_s}} u - L_{lm} dP - A_p \dot{q} \right) \quad (7)$$

where u is the control input, defined as the normalized valve spool displacement $u = x_m / x_{m,max}$.

The pressure difference dynamics of Eq. (7) represents the actuation force dynamics with the relation $F_{act} = A_q dP$. Note that as hydrostatic bearings are used in the SRS to provide smooth operation (Van Schothorst, Gert, 1997), the Coulomb friction is minimized by avoiding the metal-to-metal contact. Thus in this study, the actuator friction is considered as prismatic joint vicious friction in the platform model. Together with Eq. (1), the dynamics of the whole simulator motion system are modeled for purpose of controller design.

3. INCREMENTAL NONLINEAR DYNAMICS INVERSION(INDI)

Different from traditional control techniques, the INDI methodology calculates the increment of the control input for every sample time based on the system states one time step before, instead of computing the total control input directly (Simplício et al., 2013). Consider an n^{th} order nonlinear control inputs affined system

$$\dot{\mathbf{x}} = \mathbf{f}(\mathbf{x}) + \mathbf{G}(\mathbf{x})\,\mathbf{u} \quad (8)$$

where $\mathbf{f}$ is vector field in $\mathbb{R}^n$, $\mathbf{u} \in \mathbb{R}^m$ is the input, $\mathbf{G} \in \mathbb{R}^{n \times m}$ is the control effectiveness matrix.

In order to obtain the incremental form of the system, the system dynamics Eq. (8) are approximated by applying the first-order Taylor series expansion at the current time instant (Simplício et al., 2013):

$$\begin{aligned} \dot{\mathbf{x}} = \dot{\mathbf{x}}_0 &+ \frac{\partial}{\partial \mathbf{x}} \left[\mathbf{f}(\mathbf{x}) + \mathbf{G}(\mathbf{x})\,\mathbf{u} \right]_{\mathbf{x}_0, \mathbf{u}_0} (\mathbf{x} - \mathbf{x}_0) \\ &+ \mathbf{G}(\mathbf{x}_0)\,(\mathbf{u} - \mathbf{u}_0) \end{aligned} \quad (9)$$

The state derivatives of the system after a very small time delay are predicted based on the increments of system states and the control inputs. The zero-order term of The Taylor series $\dot{\mathbf{x}}_0$ is obtained from sensor measurements, which is why INDI is featured as a sensor-based controller. For a very small time increment, the second term of Eq. (9) is much smaller than the last term according to the principle of time scale separation (Simplício et al., 2013). The increment of states $(\mathbf{x} - \mathbf{x}_0)$ is equal to the integration of $\dot{\mathbf{x}}$, which tends to zero with infinitesimal time step, while the control input increment can still be relatively large since it is given value. The validity of this assumption requires that the dynamics of the actuators are fast enough compared with system dynamics. The incremental form of the dynamic equation is thus further simplified as

$$\dot{\mathbf{x}} = \dot{\mathbf{x}}_0 + \mathbf{G}(\mathbf{x}_0)\,(\mathbf{u} - \mathbf{u}_0) \quad (10)$$

With the above equation, the INDI control law can be designed as

$$\mathbf{u} = \mathbf{u}_0 + \mathbf{G}^{-1}(\mathbf{x}_0)\,(\boldsymbol{\nu} - \dot{\mathbf{x}}_0) \quad (11)$$

Where $\boldsymbol{\nu}$ is the virtual control input. The linear relation is then satisfied as

$$\dot{\mathbf{x}} = \boldsymbol{\nu} \quad (12)$$

As the closed loop system is now linearised, a regular linear controller can now be easily designed for $\boldsymbol{\nu}$.

In Eq. (11), no model information of $\mathbf{f}$ is required for the INDI controller, they are replaced by the state derivative measurement $\dot{\mathbf{x}}_0$. The control law is thus insensitive to model and parameter uncertainties of $\mathbf{f}$ at a cost of a dependence on state measure accuracy. As the information on the control effectiveness matrix $\mathbf{G}$ is also included in the measurement $\dot{\mathbf{x}}_0$, the control law is also insensitive to parameter uncertainties in that part of the system with a high sampling rate, even though $\mathbf{G}^{-1}$ appears explicitly in Eq. (11). This feature was analytically proven in (Simplício et al., 2013; Sieberling et al., 2010), showing that the existence of model mismatch $\Delta\mathbf{G}$ would not influence the linear relation Eq. (12), with a high sampling rate.

It is concluded that our proposed INDI control technique is capable of overcoming the model uncertainty problem for nonlinear systems, under the assumption of fast actuator dynamics, high sampling rate and accurate sensor measurements.

4. CONTROL SYSTEM DESIGN

As illustrated in Fig. 2, the main goal of the SRS simulator motion control system is to track given reference trajectory calculated online from pilot inputs and simulated aircraft model as accurately as possible. The complete control system is cascaded into an outer motion control loop and an inner hydraulic force control loop.

In this section, the control schemes for both the inner and the outer loops are discussed. This paper focuses on the inner-loop force tracking control using INDI and the design of the controller is described in detail. As a comparison, an NDI based CdP controller currently implemented in the SRS simulator is also introduced briefly. A typical force computation with a PD feedback methodology is introduced for the outer-loop motion control.

4.1 Inner-Loop INDI Controller

Controller Design Consider the hydraulic actuator dynamics given in Eq. (7) and following the procedure of the INDI methodology from Eq. (8) and (9), the first-order estimation of the pressure dynamics is given by:

$$\begin{aligned}\dot{dP} = \dot{dP}_0 &+ C_m(q_0)\Phi_n\sqrt{1-sgn(x_{m0})\frac{dP_0}{P_s}}(u-u_0)\\ &-\left[\frac{1}{2}\frac{sgn(x_{m0})C_m(q_0)\Phi_n}{\sqrt{P_s-sgn(x_{m0})dP_0}}+L_{lm}\right](dP-dP_0)\\ &-C_m(q_0)A_p(\dot{q}-\dot{q}_0)\end{aligned} \tag{13}$$

According to the time scale separation principle discussed in the previous section, the dynamic equation can be further simplified to

$$\dot{dP} = \dot{dP}_0 + C_m\Phi_n\sqrt{1-sgn(x_{m0})\frac{dP_0}{P_s}}(u-u_0)+d \tag{14}$$

where

$$d = -C_m(q_0)A_p(\dot{q}-\dot{q}_0) \tag{15}$$

The value of $\dot{dP}_0$ is obtained by numerical differentiation of the pressure sensor measurement. In practice, the noise of pressure difference measurements is significantly amplified if the signal is differentiated to obtain the derivative, thus a low-pass filter is usually applied. A simple second-order filter is adopted in the study and given by:

$$H(s) = \frac{\omega_n^2}{s^2+2\zeta\omega_n s+\omega_n^2} \tag{16}$$

In order to compensate for the delay introduced by the filter, a technique proposed in (Smeur et al., 2015) is adopted, this technique simply adds exactly the same filter as Eq. (16) in the control input memory loop, so that the measurement and the input signals are synchronized. By doing that, Eq. (14) yields

$$\dot{dP} = \dot{dP}_f + C_m\Phi_n\sqrt{1-sgn(x_{m0})\frac{dP_0}{P_s}}(u-u_f)+d \tag{17}$$

where subscript f indicates the filtered signals. The inversion of this equation for u gives the INDI control law as

$$u = u_f + G^{-1}(dP_0, u_0, q_0)\left(\nu - \dot{dP}_f\right) \tag{18}$$

where

$$G(dP_0, u_0, q_0) = C_m(q_0)\Phi_n\sqrt{1-sgn(x_{m0})\frac{dP_0}{P_s}} \tag{19}$$

Through these steps, the system is linearised and a simple linear controller is designed for the virtual control ν that the system yields

$$\dot{dP} = \nu + d \approx \nu = K_p(F_{ref}/A_p - dP) \tag{20}$$

where F_{ref} is the desired actuation force set by the outer-loop motion controller. Note that in Eq. (20) the term d is neglected since with a high sampling rate, $q \approx q_0$ holds thus $d \approx 0$ according to Eq. (15).

The final INDI control scheme is illustrated in Fig. 4 in the z-domain. The system input is the virtual control ν and the output is the pressure difference derivative $\dot{dP}$. The control input u to the valve spool is the sum of the desired increment and the last step memory through a second-order filter $H(z)$. The differentiated pressure difference measurement is filtered and fed back to be subtracted from ν for control input increment calculation. The part that represents the hydraulic actuator is based on the linearised model of Eq. (14), which in the z-domain yields

$$\dot{dP}(z)\left(1-z^{-1}\right) = G(dP_0, u_0, q_0)\,u(z)\left(1-z^{-1}\right) \tag{21}$$

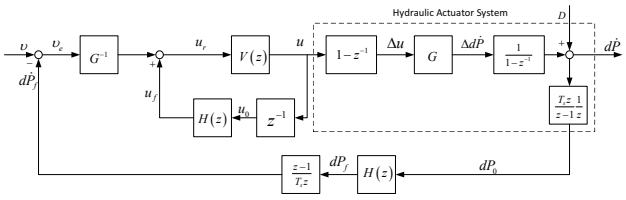

Fig. 4. INDI controller. $V(z)$ denotes the valve dynamics and $H(z)$ the second-order filter

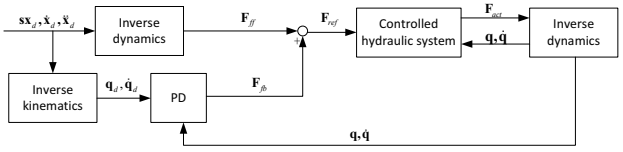

Fig. 5. Outer-loop feed forward motion controller

where the term d is also neglected. The external disturbances are represented by disturbance term D.

Note that infinitely fast valves do not exist, the dynamics of the servo-valve are included in Fig. 4 as $V(z)$. The feedback of the valve spool displacement is assumed to be available, as is the case for the SRS. If it is not the case, a model of valve dynamics are alternatively applied to predict the real spool opening u_0.

Control System Analysis Given the control diagram in Fig. 4, the transfer function in z domain of the controlled system can be calculated to analyze the influence of the introduced second-order filters. It can be easily calculated that the closed-loop transfer function of Fig. 4 is

$$\begin{aligned}\frac{\nu(z)}{\dot{dP}(z)} &= \frac{V(z)\left(1-V(z)H(z)z^{-1}\right)^{-1}}{1+V(z)\left(1-V(z)H(z)z^{-1}\right)^{-1}H(z)z^{-1}}\\ &= \frac{V(z)}{1-V(z)H(z)z^{-1}+V(z)H(z)z^{-1}}\\ &= V(z)\end{aligned} \tag{22}$$

It turns out in this equation that the valve dynamics show up in the controlled system transfer function, instead of a single integrator, as in Eq. (20). It is also verified that the introduction of the filter $H(z)$ in the control input memory loop cancels the influence of the lag it causes in the measurement feedback loop.

4.2 Inner-Loop CdP Controller

The 'cascade ΔP' (CdP) controller is a practical hydraulic force tracking technique (Heintze and van der Weiden, 1995) that is currently applied on the SRS. Considering the hydraulic actuator dynamics given by Eq. (7), the appropriate CdP control law is:

$$u = \frac{K_v\dot{q} + K_c(F_{ref}/A_pP_s - dP/P_s) + K_l dP}{\sqrt{1-sgn(x_m)\frac{dP}{P_s}}} \tag{23}$$

where the gains K_v and K_l are designed as $K_v = A_p/\Phi_n$ and $K_l = L_{lm}/\Phi_n$. Substituting this law into Eq. (7) gives:

$$\dot{dP} = 2C_m\left(q\right)K_c\Phi_n\left(F_{ref}/A_p - dP\right)/P_s \qquad (24)$$

Thus the actuator is turned into a first-order force generator with the gain varies with respect to q, that the dP will track the reference actuation force F_{ref} scaled by actuator cylinder area. The CdP controller is actually a reduced NDI controller with C_m not not inverted, hence it is sensitive to uncertainties beside this part of the model.

4.3 Outer-loop motion controller

The outer-loop motion tracking control scheme used in this study matches the implementation on the SRS. As depicted in Fig. 5, the control input is composed of a feedforward term and a linear feedback term. The feedforward forces $\mathbf{F}_{ff}$ are calculated based on the reference trajectory given in operation space and the inverse dynamics of the system:

$$\mathbf{F}_{ff} = \mathbf{H}^{-1}\mathbf{M}\left(\mathbf{sx}_d\right)\ddot{\mathbf{x}}_d + \mathbf{H}^{-1}\boldsymbol{\eta}\left(\dot{\mathbf{x}}_d, \mathbf{sx}_d\right) \qquad (25)$$

In addition, a PD feedback loop is implemented in the joint space to stabalize the system:

$$\mathbf{F}_{fb} = \mathbf{K}_P\left(\mathbf{q}_d - \mathbf{q}\right) + \mathbf{K}_D\left(\dot{\mathbf{q}}_d - \dot{\mathbf{q}}\right) \qquad (26)$$

where the desired actuator length $\mathbf{q}_d$ and velocity $\dot{\mathbf{q}}_d$ are calculated through simple inverse kinematics from the given motion reference.

5. SIMULATION RESULTS

The INDI force controller developed in Section 4 as well as the NDI based CdP controller will next be used for motion control of a complete hydraulic hexapod flight simulator, cooperating with the aforementioned outer-loop motion controller in a cascaded structure. A well-validated and fully nonlinear simulation model (Van Schothorst, Gert, 1997; Huang et al., 2016b) of the SRS is used for the simulations.

The motion profile of a real-world experiment on the SRS (Miletović et al., 2016) is chosen as the reference trajectory of the motion system. This profile moves the upper platform periodically along a circular path in the horizontal plane with a radius of 0.5 meters and a period of five seconds after a brief lead-in period (Huang et al., 2016b).

For all the simulations, the system dynamics are updated at 5000 Hz. The inner-loop controllers are sampled at 5000 Hz and the outer-loop controller at 1000 Hz. The linear gains of the outer-loop controller are set to be $K_p = 8\times10^5$ and $K_d = 3\times10^3$. Nominal oil supply pressure is set to 160 bar, white noises are added to the pressure difference feedback as a simulation of measurement noises. Only the simulation results of actuator 1 and actuator 3 are presented for brevity.

5.1 Performance at Nominal Condition

Performances of INDI and CdP approaches under nominal conditions are first compared. Fig. 6 presents the force tracking errors of both controllers, which are normalized by A_pP_s. The manoeuvre starts from 15 s after a preparation stage, during which the platform moves from the neutral position to the initial position from 5 s to 10s. The root-mean-squared errors of INDI are 0.0034 and 0.0035 for actuators 1 and 3, which are much better than the 0.016 and 0.018 for the NDI-based CdP controller. The influence of noise is noticeable but the performance is not hardly affected. The relative big errors for CdP are caused by the fact that in order to get the expression for the hydraulic pressure dynamics (Eq. (7)), small terms in Eq. (4) are neglected and geometrically ideal valve is assumed, which means a certain degree of unmodeled dynamics exist in Eq. (7). Hence even nominal parameters are used, the CdP controller does not precisely invert the full nonlinear dynamics and the performance is degraded. INDI controller is notably more robust to these unmodeled dynamics.

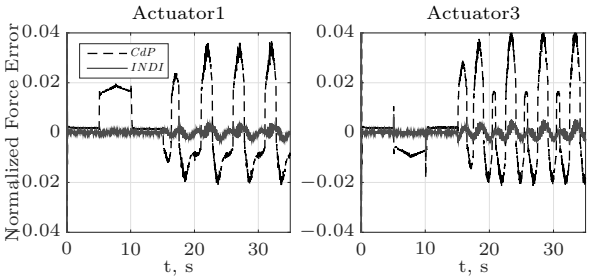

Fig. 6. Nominal force tracking errors

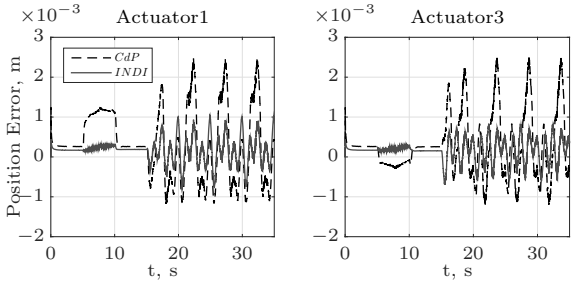

Fig. 7. Nominal position tracking errors

Fig. 7 shows the actuator position errors of the same simulation. It is clear that errors with the INDI controller are significantly smaller than those attained with of the CdP controller. This indicates that the improved inner-loop force tracking performance with INDI controller contributes to the overall control performance significantly.

5.2 Robustness Test

One of the most important parameters in Eq. (7) is the nominal valve flow Φ_n, for which an accurate valve is hardly accessible due to valve spool gaps, opening overlaps and manufacturing errors. Thus the robustness of the force controller against any modeling error is of importance. Fig. 8 shows the performance of both controllers for actuator 1 and 3 with 50% and 20% parameter mismatches in terms of Φ_n. It is clear that the CdP controller is highly sensitive to the parametric uncertainty of Φ_n. With a mismatch greater than 20%, the performance is significantly deteriorated. With the same setting of parameter mismatch, the performance of INDI-controlled system is almost intact as the parameter mismatch level increases, while that of the CdP approach is significantly degraded. This result thus proves the robustness of INDI controller as analyzed in Sections 3 and 4.

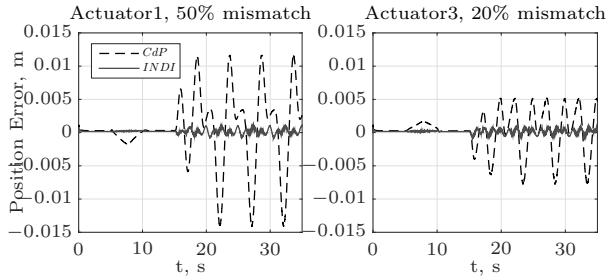

Fig. 8. Position tracking errors with parameter mismatch

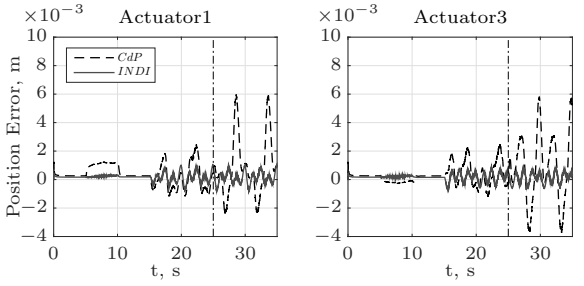

Fig. 9. Position tracking errors with pressure decrease

As flight simulators are generally well protected with a safe working space, not much external disturbances are likely to act on such systems. However, some perturbations are still considered such as the sudden change of oil supply pressure P_s. Thus the robustness of the force controller against P_s is still of concern. Fig. 9 presents the position error of each leg with both control schemes when facing a decrease in supply pressure. Both controllers start with a nominal supply pressure $P_s = 160\ bar$ and after 25 s the supply pressure is suddenly decreased by 20%. It is shown that the CdP controller suffers from the pressure change and the performance is significantly degraded, while the performance of INDI controller remains intact. The robustness of the INDI approach is further verified by this result.

It is also clearly illustrated by the above results that INDI is inherently not sensitive to non-control-related parameters such as L_{lm}, since they do not appear in the control law at all.

6. CONCLUSIONS

INDI control is a very promising technique for inner-loop control of high performance hydraulic hexapod flight simulators. By improving the force tracking performance for each nonlinear hydraulic actuator and introducing a stable outer-loop controller, the overall motion performance can be greatly improved. Compared with traditional NDI-based CdP controller, the INDI approach needs less model information while offering better performances hence typical motion controllers for parallel robots can be easily applied to hydraulic driven systems.

In terms of robustness, INDI is not sensitive to almost all types of model uncertainties, which is notably usable for hydraulic driven systems since accurate model parameters are hardly available and even time-variant. As a trade-off, the INDI is sensitive to the quality of state measurements. However filters are useful for deal with sensor noises. The INDI controller is also promising for better performance of other applications of hydraulic driven robots.

REFERENCES

Alleyne, A., Liu, R., and Wright, H. (1998). On the Limitations of Force Tracking Control for Hydraulic Active Suspensions. In *American Control Conference*, June, 43–47.

Chin, J.H., Sun, Y.H., and Cheng, Y.M. (2008). Force computation and continuous path tracking for hydraulic parallel manipulators. *Control Engineering Practice*, 16(6), 697–709.

Dasgupta, B. and Mruthyunjaya, T.S. (1998). Closed-Form Dynamic Equations of The Ceneral Stewart Platform Through The Newton-Euler Approach. *Mechanism and Machine Theory*, 33(7), 993–1012.

Heintze, J. and van der Weiden, A. (1995). Inner-loop Design and Analysis for Hydraulic Actuators, With an Application to Impedance Control. *Control Engineering Practice*, 3(9), 1323–1330.

Huang, Y., Pool, D.M., Stroosma, O., Chu, Q.P., and Mulder, M. (2016a). A Review of Control Schemes for Hydraulic Stewart Platform Flight Simulator Motion Systems. In *AIAA Modeling and Simulation Technologies Conference*.

Huang, Y., Pool, D.M., Stroosma, O., Chu, Q.P., and Mulder, M. (2016b). Modeling and Simulation of Hydraulic Hexapod Flight Simulator Motion Systems. In *AIAA Modeling and Simulation Technologies Conference*.

Koekebakker, S. (2001). *Model Based Control of a Flight Simulator Motion System*. Ph.D. thesis, Delft University of Technology.

Merritt, H.E. (1967). *Hydraulic Control Systems*. John Wiley & Sons.

Miletović, I., Stroosma, O., Pool, D.M., van Paassen, M.M., and Chu, Q.P. (2016). Improved Stewart Platform State Estimation using Inertial and Actuator Position Measurements. *Control Engineering Practice (under review)*.

Sieberling, S., Chu, Q.P., and Mulder, J.A. (2010). Robust Flight Control Using Incremental Nonlinear Dynamic Inversion and Angular Acceleration Prediction. *Journal of Guidance, Control, and Dynamics*, 33(6), 1732–1742.

Simplício, P., Pavel, M.D., Van Kampen, E., and Chu, Q.P. (2013). An Acceleration Measurements-Based Approach For Helicopter Nonlinear Flight Control Using Incremental Nonlinear Dynamic Inversion. *Control Engineering Practice*, 21, 1065–1077.

Smeur, E.J.J., Chu, Q.P., and de Croon, G.C. (2015). Adaptive Incremental Nonlinear Dynamic Inversion for Attitude Control of Micro Aerial Vehicles. *Journal of Guidance,Control, and Dynamics*, 38(12), 450–461.

Stewart, D. (1965). A platform with six degrees of freedom. *Proceedings of the Institution of Mechanical Engineers*, 180(1), 371–386.

Stroosma, O., Van Paassen, R., and Mulder, M. (2003). Using the SIMONA Research Simulator For Human-Machine Interaction Research. In *AIAA Modeling and Simulation Technologies Conference and Exhibit*, 5525.

Van Schothorst, Gert (1997). *Modelling of Long-Stroke Hydraulic Servo-Systems for Flight Simulator Motion Control and System Design*. Ph.D. thesis, Delft University of Technology.